



## Reduction characteristics of disinfection by-product (DBPs) generated by allogenic organic matter (AOM) using micro-hollow beads in terms of particulate removal

Minsoo Maeng, Nirmal Kumar Shahi, Seok Dockko\*

Department of Civil and Environmental Engineering, Dankook University, 152, Jukjeon-ro, Suji-gu, Yongin-si, Gyeonggi-do, 16890, Korea, email: dockko@dankook.ac.kr (S. Dockko), minsoo13@dankook.ac.kr (M. Maeng), nirmalshahi143@gmail.com (N.K. Shahi)

Received 20 May 2019; Accepted 21 September 2019

### ABSTRACT

Allogenic organic matter (AOM) removal technologies using micro-hollow beads have been developed. Micro-hollow beads with low density ( $0.125 \text{ g/cm}^3$ ) were found to be effective for the flotation in terms of particulate matter removal. To investigate the characteristics of AOM, extracellular organic matter (EOM), and intracellular organic matter (IOM) before and after chlorine injection, the effect of molecular weight distribution on liquid chromatography with organic carbon detection was examined. The chromatography dissolved organic carbon values of EOM and IOM were 7.5 and 1.6 mg/L, respectively, and the compositions of building blocks and humic substances of EOM and IOM were 58% and 20%, respectively. A particle counter was used to confirm the reduction in the number of residual particles by micro-hollow beads. The concentration of particulate matter decreased with a higher concentration of micro-hollow bead injection due to the attachment and flotation of micro-hollow beads to particulate matter. By removing precursors of the disinfection by-products (DBPs), micro-hollow beads were able to reduce the concentration of DBPs and DBPFP. Haloacetic acids (HAAs) were converted to particulate material through a chlorination process rather than through trihalomethanes (THM) and are efficiently removed by the micro-hollow beads. Compared with THMs/total organic carbon (TOC), HAAs/TOC showed better removal characteristics. THMFP concentrations remained constant over time, whereas HAAFP and HANFP values increased with retention time. Over 7 d of reaction, THMFP and HANFP showed no change in constituents, but HANFP was detected as TCAN, DCAN, and DBAN.

*Keywords:* Micro-hollow beads; Allogenic organic matter (AOM); Disinfection by-products (DBPs); Liquid chromatography with organic carbon detection (LC-OCD); Particulate removal; Precursors

### 1. Introduction

Allogenic organic matter (AOM) as by-products from the algal cell composed of proteins, neutral and charged polysaccharides, nucleic acids, lipids, and small molecules, which are considered as intracellular organic matter (IOM) and excretion from the metabolic activity and autolysis are considered as extracellular organic matter (EOM) [1,2].

Especially during dry seasons, approximately 50% of the total dissolved organic matter (DOC) in surface water is reported to be contributed from AOM [3]. Upon chlorination, algal cell lysis results in an exponential increase in EOM and IOM in drinking water treatment plants (DWTPs). Further, the reaction of chlorine with precursors from cell lysis results in the formation of undesirable carbonaceous and nitrogenous disinfection by-products (C- and N-DBPs) [4,5].

\* Corresponding author.

The C-DBPs such as trihalomethanes (THMs) and haloacetic acids (HAAs) and N-DBPs such as haloacetonitriles (HANs) and halonitromethanes (HNMs) are reported at high concentration in DWTPs and potential human carcinogens [6]. Moreover, N-DBPs are more cytotoxic and genotoxic than C-DBPs [7,8], which occurred more often when IOM reacts with chlorine. Since IOM has precursors that contribute to more DBPs formation than EOM, it is recommended that AOM to be removed before the chlorination. AOM is also supposed to hinder the coagulation and sedimentation process [2,9,10]. Since the algae have a characteristic of floating, the treatment efficiency is not high due to poor sedimentation. Thus, there is a possibility that precursors contributing to total organic carbon (TOC) and total nitrogen (TN) may not achieve sufficient removal efficiency. Therefore, TOC and TN including particulate matters were significant parameters for THMs, HAAs, and HANs. To investigate the removal characteristics of precursors after chlorine injection, the removal tendency of high and low-molecular substances of algae after coagulant injection can be found through liquid chromatography-organic carbon detection (LC-OCD) analysis [11,12]. This is because the amount of DBP formation can be detected differently for each molecular size [13,14]. The coagulation and sedimentation process have known to be the conventional method for destabilizing the algae and enhancing algal removal. However, dissolved air flotation (DAF) in respect of particle separation is a more effective process for the removal of blue-green and green algae [15,16]. DAF can remove more than 90% of *Microcystis aeruginosa* with optimal coagulant dosage [17]. Previous studies compared the production of C-DBPs and N-DBPs from DAF and a conventional gravity system (CGS) used for the removal of algae before and after chlorine injection [2,18]. However, DAF is economically burdensome because of its high-energy consumption. Thus, a method to address the low energy efficiency has developed, namely AOM removal technologies using micro-hollow beads in terms of particulate removal [19,20]. Therefore, in conventional water treatment plants based on sedimentation, micro-hollow beads that can be applied effectively for particle removal are being sought as an alternative to high turbidity and algae removal. Micro-hollow beads were able to make the attached flocs floatable to remove algal in the testbed. *Microcystis aeruginosa* has pores in its cells that trap air in the cells, making them floatable in water [21]. The low-density characteristic of micro hollow beads can assist removal by floating particulate matter in conjunction with the floating characteristics of the algae. As mentioned above, insufficient removal efficiency obtained by sedimentation can be increased using micro-hollow beads. In terms of effective particle removal, there is a possibility to reduce the generation of DBPs using micro-hollow beads.

The purpose of this work was to identify the removal efficiency of DBPs using micro-hollow beads. First, LC-OCD was used to analyze the configuration and MW of AOM, which was divided into EOM and IOM. The MW change in the organic material before and after disinfection was also measured. Second, particle size analysis was also conducted to verify the effects of the micro-hollow beads on particulate organic matter and precursor removal. Third, the effects of DBP removal through the addition of polyaluminum

chloride (PAC) and micro-hollow beads were investigated. Lastly, the effects of retention time and micro-hollow bead injection on DBPFP formation were verified.

## 2. Materials and methods

### 2.1. Micro-hollow beads and coagulant

Micro-hollow beads (3M Co., Maplewood, USA) that were washed with distilled water to remove contaminants were used for the experiment. This washing was the pre-treatment process to remove micro-hollow beads that float weakly; this process reduces experimental error and increases the floating efficiency. Micro-hollow beads have a low density of 0.125 g/cm<sup>3</sup> because of the presence of pores inside. Table 1 shows the properties of the micro-hollow beads, with an average size of 50 μm and an internal thickness of 200 nm. The coagulant used in this experiment was (PAC 10%; Hongwon Industry, Busan, Korea).

### 2.2. Algae cultivation and raw water

*Microcystis aeruginosa* used as AOM was cultivated by K-water and subcultivation in the laboratory. *Microcystis aeruginosa* was subcultured in a sterilized BG-11 medium prepared in the laboratory [2]. The BG-11 medium was sterilized by autoclaving at 121°C for 30 min with a pH of 7.0 prior to use. After cooling at room temperature, the BG-11 was used as a medium. To grow *Microcystis aeruginosa* in the lab, the cultivation performed base on 24 h light with temperature 27°C. Air was supplied for 24 h. All samples were mixed homogeneously by horizontal-type digital reciprocating shaker (Daihan Scientific Co., Wonju, Korea). The cells were harvested at an exponential growth phase (cell count, 3.2 × 10<sup>7</sup> cells/mL). The cell count was conducted using photography with an optical microscope (Eclipse E200, Nikon, Minato, Japan) using hemocytometers. The characteristics of *Microcystis aeruginosa* used as AOM (diluted six times) were analyzed in the laboratory and are shown in Table 2. The SUVA value was 3.96, which is close to that of hydrophobic material, which can be generally removed through the coagulation process. The TN showed higher concentration than TOC, indicating the possibility of nitrogen DBPs. On the other hand, EOM was extracted by centrifuging harvested cell culture at 5,000 rpm for 15 min and obtained supernatant was filtered through a 0.45 μm filter. The settled algae cells in the centrifuge tube were washed twice with deionized water and resuspended. The cells were then subjected to three cycles of freezing (−20°C) and thawing (35°C) to induce cell lysis. Next, the solution was centrifuged

Table 1  
Property of micro-hollow beads

Items	Values
Pressure (psi)	250
Fractional survival (%)	90
Density (g/cm <sup>3</sup> )	0.125
Conductivity (s/m)	0.047
Average particle size (μm)	50

Table 2  
Characteristics of *Microcystis aeruginosa*

Parameters	Values
Turbidity (NTU)	8.36
TOC (mg/L)	3.24
TN (mg/L)	22.1
UV <sub>254</sub> (cm <sup>-1</sup> )	0.125
SUVA (L/mg m)	3.96
Counts/cell	3.2 × 10 <sup>7</sup>

at 10,000 rpm for 15 min, and the supernatant was filtered through a 0.45 µm filter to obtain IOM [2,7]. DOC value for both EOM and IOM was measured and compared with previous studies [5,22,23]. The variation in DOC concentration might be due to different environmental conditions for culture and exponential growth phase. The values are illustrated in Table 3.

### 2.3. LC-OCD analysis

The LC-OCD (DOC-Labor Dr. Huber, Germany) composes with a sample injector, a size exclusion chromatography column, a thin-film reactor, a UV<sub>254</sub> detector, and a nondispersive infrared detector. The MW fractions of organic matter consists of biopolymers (>20,000 g/mol), humic substances (1,000–20,000 g/mol), building blocks (350–1,000 g/mol), low-MW (LMW) acids (350 g/mol), and LMW neutrals (<350 g/mol) [2]. MW distribution about AOM can be useful in understanding the importance of DOC and SUVA values because different MW fractions could behave differently in water treatment plants [14]. To analyze the removal characteristics of organic fractions based on their MW of EOM, IOM,

Table 3  
Measured value of DOC from EOM and IOM

EOM (mg/L)	IOM (mg/L)	Days	Cell count/mL	References
29.7	100.5	na	2 × 10 <sup>8</sup>	[22]
4.4	3.6	na	na	[23]
na	3.0	20–28	na	[24]
14.0	5.5	14	3.2 × 10 <sup>7</sup>	Present Study

Note: na is not available.

and AOM, LC-OCD analysis was carried out. EOM, IOM, and AOM were analyzed before and after chlorine injection to investigate the change characteristics by MW [2,3,24]. The removal efficiency was examined in MW fractions.

### 2.4. Particle counting method

The digital online particle counter monitor (PCM) (PC 2400 D, Chemtrac, Norcross, USA) was used in the experiment, as shown in Fig. 1. The measurement ranges were used with nine channels. The particle size was measured from 2 to 100 µm. The sample flow rate was adjusted to 100 mL/min to measure the number of particles in 100 mL of the sample using a master flux pump. Each time the sample was replaced, the tube was cleaned with distilled water. The data was used when it was recorded reliably.

### 2.5. Experimental setup and operating conditions

Coagulation and flocculation experiments were conducted with a standard jar tester (Philips Bird's, Richmond, USA). Acrylic jars 100 mm in diameter and 200 mm in height

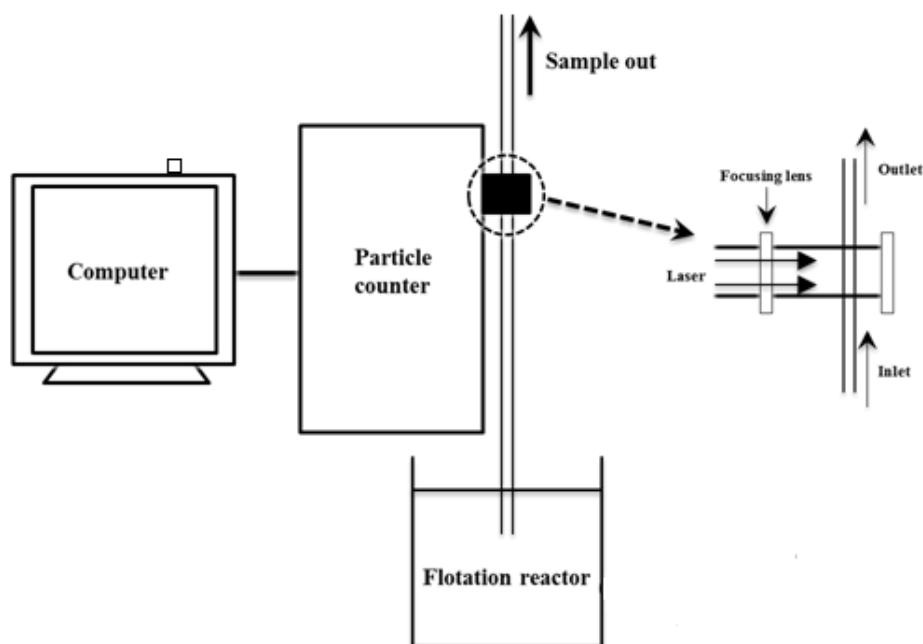


Fig. 1. Schematic diagram of the particle counting method.

had a valve at 10 mm and another valve at 40 mm from the bottom of the jar. Micro-hollow beads were injected after 30 s of mixing at 150 rpm after PAC injection. Coagulation and flocculation were conducted through rapid mixing (150 rpm for 1 min) and slow mixing (30 rpm for 5 min). The optimal flotation conditions were verified by changing the PAC and micro-hollow bead concentrations. The PAC was injected in 0, 5, 10, and 20 mg/L, where beads were tested with concentrations of 10, 30, 60, and 100 mg/L. With chlorine injection experiments, precursors were tested under chlorine concentrations of 1, 3, 5, and 10 mg/L for 1 h. All reactors were adjusted to pH  $7.0 \pm 0.5$  using 0.1 N NaOH and 0.1 N HCl.

## 2.6. DBP formation

A stock solution of 1,000 mg/L as chlorine was prepared to oxidize organic matters. Oxidation of the organic matter was performed by injecting different chlorine concentrations (1, 3, 5, and 10 mg/L) and pH was adjusted to  $7.0 \pm 0.5$  using 0.1 N NaOH and 0.1 N HCl. The formation of potential experiments were conducted after 1, 3, 5, and 7 d. To prevent further reaction of chlorine with organic matters before the analysis of THMs, all the samples were acidified by ascorbic acid and quenched with 1 + 1  $H_3PO_4$ . In addition,  $Na_2HPO_4$  and  $KH_2PO_4$  were used to prevent residual chlorine reaction before the analysis of HANs and HAAs [25].

## 2.7. Analysis

The TOC measurements were made by a TOC analyzer (TOC-L, Shimadzu Co., Japan). The TN was analyzed by a UV spectrophotometer (DR 5000, Hach Co., USA). The concentration of THMs was analyzed using gas chromatography-mass spectrometry (Purge and Trap, Agilent Co., USA), and the concentrations of HAAs and HANs were analyzed using gas chromatography with electron capture detection (Agilent Co., USA).

## 3. Results and discussion

### 3.1. LC-OCD analysis

#### 3.1.1. MW distribution of AOM by LC-OCD

AOM has low aromaticity with high organic nitrogen material and is mainly hydrophilic rather than hydrophobic. AOM contains DBP precursors. Therefore, when algal matter inflows to DWTPs, chlorine should not be used. Table 4 shows that organic fractions contributed by EOM

Table 4  
Organic fractions contributed by EOM and IOM extracted from AOM [2]

CDOC	EOM	IOM
Biopolymer (mg/L)	1.319	0.347
Building blocks and humic substances (mg/L)	4.471	0.336
LMW neutrals (mg/L)	1.504	0.961
LMW acids (mg/L)	0.333	0.120

and IOM extracted from AOM [2]. Throughout the whole MW distribution, EOM showed higher chromatography dissolved organic carbon (CDOC) than IOM. Although the CDOC of IOM exists in lower concentrations than that of EOM, the concentrations of by-products such as THMs, HAAs, and C-DBPs are greater [5] because of the elution of IOM by the reaction with chlorine, which produces more DBPs than EOM [26]. Fig. 2. shows the LC-OCD analysis of IOM and EOM as well as AOM and illustrates how chlorine influences algal organic matter based on the MW. Fig. 2a shows the accumulative CDOC values of EOM and IOM at 7.5 and 1.6 mg/L, respectively; thus, the CDOC value of EOM is five times that of IOM. The compositions of building blocks and humic substances of EOM and IOM are 58% and 20%, respectively. Biopolymer, building blocks and humic substances composed of high MW were mainly distributed in EOM, and LMW neutrals were distributed in IOM. Most of the DBPs produced from IOM were likely to occur in LMW neutrals (0.9 mg/L). Fig. 2b shows the EOM, IOM,

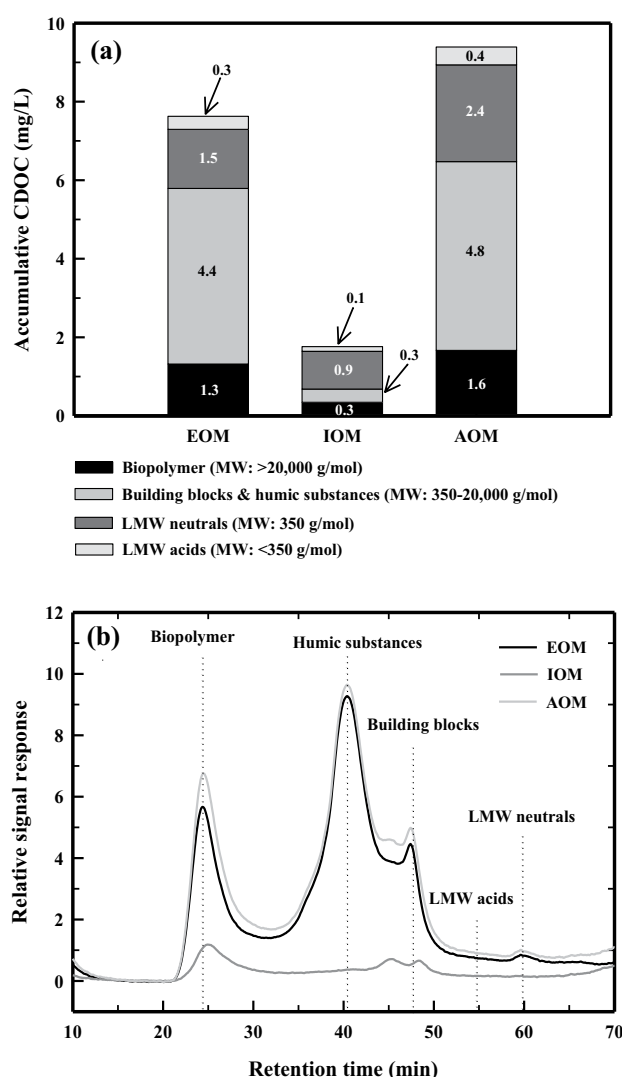


Fig. 2. Organic distribution of MW in EOM, IOM, and AOM. (a) Accumulative CDOC mg/L and (b) relative signal response.

and AOM characteristics per MW based on the retention time of the LC-OCD. EOM showed higher compositions of building blocks and humic substances, while IOM showed higher LMW nutrient concentration. High MW EOM and IOM materials were observed to be highly removed at >20,000 g/mol. The building blocks and humic substances that produce more DBPs showed higher removal with EOM. Previously, EOM was reported to show higher removal with both CGS and DAF treatment [2], indicating that EOM is easier to remove than IOM, resulting in lower by-product formation. However, the building blocks and humic substances ratio of the IOM showed lower removal, resulting in a substantial amount of DBP formation.

### 3.1.2. MW distribution of AOM according to chlorine injection

Fig. 3 shows the effect of 10 mg/L of chlorine on AOM distribution after the CGS and DAF treatment. A and B showed the results from the CGS before and after chlorine injection. The biopolymer amount in A was higher than B because the biopolymer reaction of B with chlorine converted it to lower MW matter. DAF treatment also showed similar results in C and D to those of CGS. Biopolymers showed high removal with coagulation processes, resulting in CDOC with lower MW [27]. Building blocks and humic substances showed higher CDOC concentrations before chlorine treatment, as seen with biopolymers. However, the LMW neutrals and LMW acids showed higher CDOC concentrations after the chlorine treatment. As noted, the high-MW biopolymer and building blocks and humic substances were decomposed to form LMW neutrals and LMW acids. Additionally, the CDOC values increased with CGS and DAF treatment after the chlorine processes

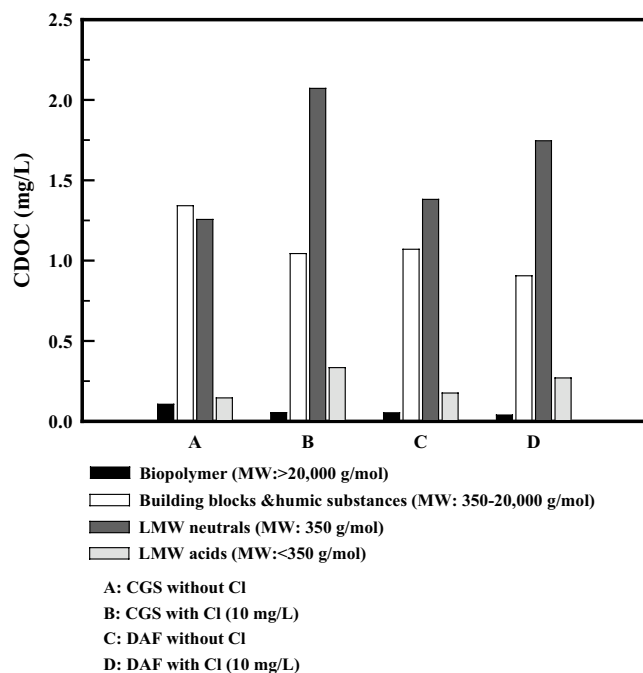


Fig. 3. MW distribution of AOM with and without chlorine injection.

because of the low treatment of LMW substances such as the hydrophobic substances.

### 3.2. PCM analysis of AOM with and without chlorine injection

The optimal concentration of micro-hollow beads was tested with PAC 10 mg/L. Fig. 4a shows the number of particles according to the concentration of micro-hollow beads. With the addition of micro-hollow beads, the average particle size was <15  $\mu\text{m}$ , and the number of particles increased with smaller particle sizes. With the addition of 10, 30, 60, and 100 mg/L of micro-hollow beads, the numbers of particles with a diameter of 3.5  $\mu\text{m}$ , the smallest particle measurable, were 1,250; 1,115; 656; and 601 counts/mL, respectively. Given that similar particle numbers were observed in samples with concentrations of 60 and 100 mg/L, the optimal dose of micro-hollow beads was selected as 60 mg/L to reduce operating costs. Fig. 4b shows the total number of particles and the average size of particles according to the various concentrations. It is clear that the higher the concentration of micro-hollow beads, the smaller the number of particles. This relationship resulted from the attachment and flotation of micro-hollow beads to particulate matter. The average size of particles slightly decreased with a greater concentration of micro-hollow beads, showing that the addition of beads did not strongly influence the size of the particulate matter. However, because of the removal of large particulate matter, the micro-hollow beads influenced the average size of the particulate pollutants. Fig. 4c shows the average particle size according to the concentration of chlorine when the micro-hollow bead concentration is 60 mg/L. After the chlorine reaction, most of the particles consisted of diameters <3.5  $\mu\text{m}$ . With chlorine concentrations of 1, 3, 5, and 10 mg/L, the concentrations of particles with a diameter of 3.5  $\mu\text{m}$  were 450, 352, 182, and 77 counts/mL, respectively. Particle sizes decreased with increased chlorine concentrations because of the chlorine decoloring or reduction in organic particulate matter. Comparing the results with the samples without chlorine treatment, the samples with chlorine treatment had 2.7 times fewer particles with a diameter of 3.5  $\mu\text{m}$  than the samples without chlorine treatment. Because of the chlorine, the particulate organic matter reduced to smaller sizes. Fig. 4d shows the total particle concentration and average particle size based on the chlorine concentration. In the chlorine concentrations of 3 and 10 mg/L, the number of particles was greatly reduced compared with the untreated samples. At concentrations of 10 mg/L, the total number of particles was 101 counts/min. For organic particles <3.5  $\mu\text{m}$ , the interaction with chlorine converts the particulate matter to dissolved forms. Thus, compared with the untreated samples (Fig. 4b), adding chlorine increased the average particle size of the particulate matter.

### 3.3. Effect of DBPs according to micro-hollow bead dose

#### 3.3.1. Precursors of C-DBPs and N-DBPs

The AOM precursors that can produce C-DBPs and N-DBPs are separately distinguished as TOC and TN, respectively. Fig. 5a shows the TOC and TN concentrations

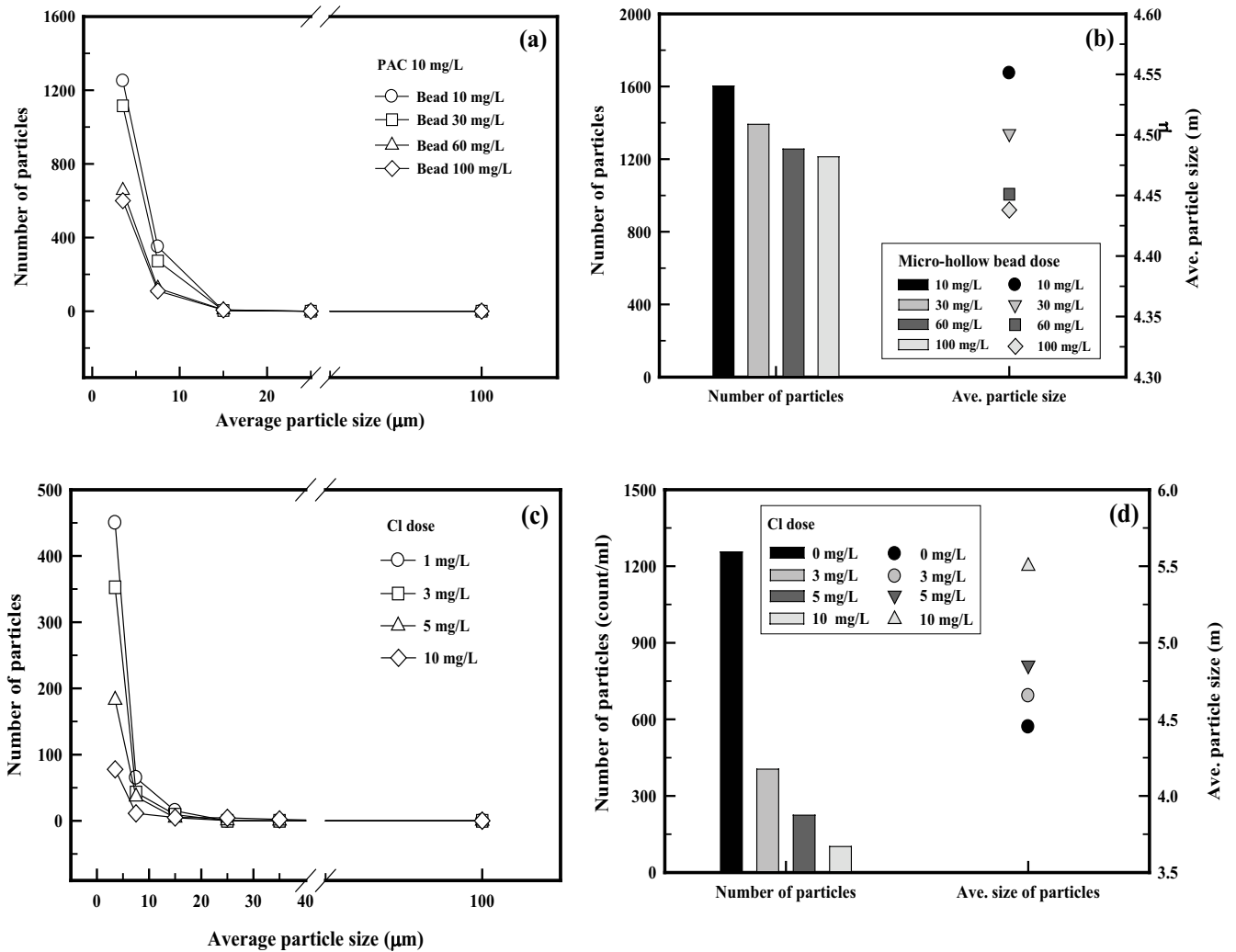


Fig. 4. Number of particles and size according to micro-hollow beads. (a) Number of particles on micro-hollow beads, (b) the total number of particles on micro-hollow beads, (c) number of particles with Cl dose, and (d) the total number of particles on Cl dose.

based on the concentrations of micro-hollow beads with PAC 10 mg/L. The TN concentration was higher than the TOC concentration. However, the removal rate of TOC was higher than that of TN because the micro-hollow beads were more effective in removing the flocs containing TOC. Additionally, during the coagulation/flocculation process, TOC showed a higher removal rate than TN matter [18]. Although the removal rate of TOC is greater than that of TN, it is necessary to confirm the concentrations and removal rates of THMs, HAAs, and HANs in terms of DBP removal. When injecting a large concentration of micro-hollow beads, the removal rates of TOC and TN were not affected. For economical and effective results, it is important to know the appropriate injection concentration of the micro-hollow beads. Fig. 5b shows how the TOC/TN concentration ratio affects the removal rates of THMs, HAAs, and HANs. Although THMs were detected to have the highest concentration, the TOC removal rate was the lowest and the removal rate of HAAs was the highest. As TOC/TN increased, the removal rate of THMs decreased, and HAAs and HANs showed a similar removal rate.

The highest DBP removal rates were observed at low TOC/TN; THMs, HAAs, and HANs were detected at 57%, 96%, and 90%, respectively. The removal rate of THMs showed a relatively high trend when the TOC/TN rate was low. However, HAAs and HANs did not cause any significant changes. Overall, the concentration of HAAs was higher than that of HANs, and the removal rate of HAAs was also higher.

### 3.3.2. Reduction of DBP micro-hollow bead dose

The effect on micro-hollow bead injection according to DBPs is shown in Fig. 6. DBPs were generated under PAC 10 mg/L and chlorine 10 mg/L. THMs showed a higher generation than HAAs and HANs in environments without and with beads. The concentrations of THMs in environments without and with beads were 230 and 75  $\mu\text{g/L}$ , respectively, whereas the concentration of HAAs decreased from 49 to 4.6  $\mu\text{g/L}$  and that of HANs from 11 to 7  $\mu\text{g/L}$ . The micro-hollow beads were demonstrated to influence the DBPs from both TOC and TN matter.

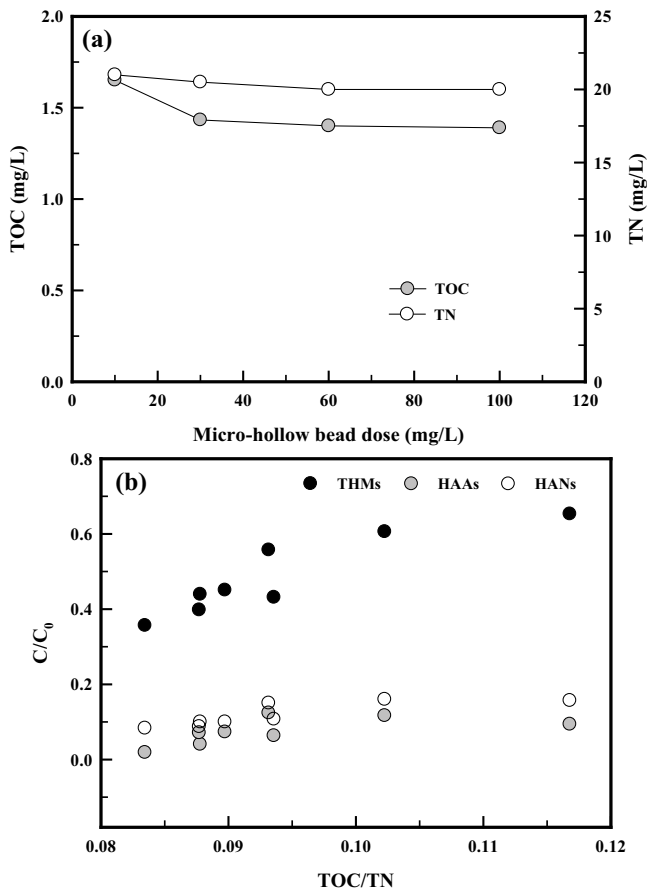


Fig. 5. Effect of precursors according to micro-hollow bead dose. (a) TOC and TN using micro-hollow beads and (b) DBPs by TOC/TN.

### 3.4. Effect of DBPs according to chlorine and PAC

Fig. 7 shows the effect of TOC and TN used as precursors on THMs, HAAs and HAN formation. The generation trends of THMs/TOC, HAAs/TOC, and HANs/TN were verified in environments with micro-hollow bead 60 mg/L and by changing the chlorine and PAC concentrations. Fig. 7a shows the THMs/TOC generation based on the PAC and chlorine concentrations. With PAC 5 mg/L and a chlorine 5 mg/L, the THMs/TOC increased continuously. However, with a PAC 10 mg/L and chlorine 5 mg/L, THMs/TOC showed constant values of 45  $\mu\text{g/L}$ . With PAC 5 mg/L and chlorine 10 mg/L, the THMs/TOC removal rate was 26.0%. With PAC 10 mg/L and chlorine 10 mg/L, it was 37.0%. Consequently, PAC 5 mg/L was not the optimum dose of coagulant. THMs/TOC showed a tendency to increase continuously because the DBP's precursor for contacting Cl remained in the treated water. However, in samples with chlorine 5 mg/L and PAC 10 mg/L, the concentration of THMs/TOC remained almost constant. The concentration of the coagulant in the removal of THMs was considered to have a significant effect. THM/TOC was able to lower the concentration by removing the TOC by adding micro hollow beads at the optimum coagulant injection. Fig. 7b shows the HAAs/TOC formation with various chlorine and

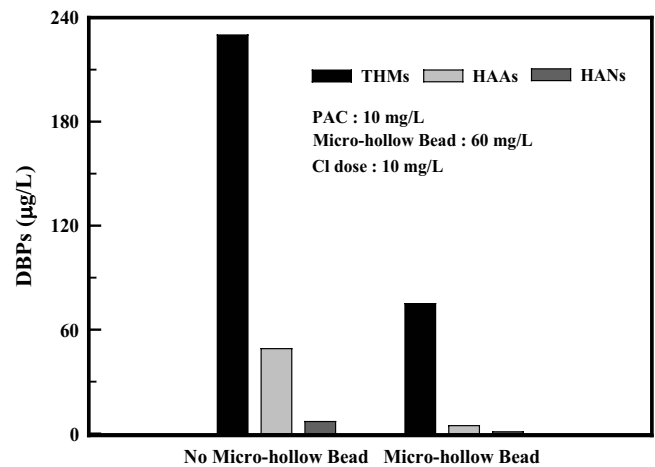


Fig. 6. Removal tendency of DBPs before and after micro-hollow bead dose.

PAC concentrations. The results showed a similar trend as with THMs/TOC formation. However, although PAC was not injected (PAC 0 mg/L), concentrations of HAAs/TOC were reduced by Cl concentration injection compared with the concentrations of THMs/TOC because the HAAs are converted to a particulate material through the chlorination process rather than THM and is efficiently removed by the micro-hollow beads. With PAC 5 mg/L and chlorine 10 mg/L, the HAAs/TOC removal rate was 41.5%. With a PAC 10 mg/L and chlorine 10 mg/L, it was 60.4%. Compared with THMs/TOC, HAAs/TOC showed better removal characteristics. However, with respect to the total quantity, THMs showed higher removal rates compared with HAAs. Fig. 7c shows the HANs/TN formation under various PAC and chlorine concentrations. The concentration of HANs/TN with Cl did not increase significantly but only tended to increase slightly. Thus, the concentration of HANs is likely to increase continuously depending on the reaction time of the chloride. In chlorine 10 mg/L, The HANs/TN removal rates of PAC 5 and 10 mg/L were 52.6% and 64.7%, respectively. With the low formations of HANs/TN, HANs/TN removal was higher than that of THMs/TOC and HAAs/TOC. Toxins from N-DBPs were 60 times more toxic than C-DBPs, thus leading to higher interest in the formation [18].

### 3.5. Reduction of DBPFP according to the retention time of chlorine

#### 3.5.1. Effect of DBPFP by Cl retention time

Fig. 8 shows the long-range effect of chlorine in the formation of THMFP, HAAFP, and HANFP from AOM. The THMFP, HAAFP, and HANFP concentrations showed increased formation with chlorine contact under micro-hollow beads 60 mg/L and PAC 5 mg/L due to the residual C-DBP and N-DBP from the non-optimal PAC concentrations. Under PAC 5 mg/L, THMFP formation after 1 and 7 d was 83.9 and 132.7  $\mu\text{g/L}$  respectively, which represented an increase of over 1.5 times. Additionally, HAAFP and HANFP showed concentrations of 8.3 and 4.5  $\mu\text{g/L}$  after 1 d, respectively. These were detected at 10.1 and 6.5  $\mu\text{g/L}$

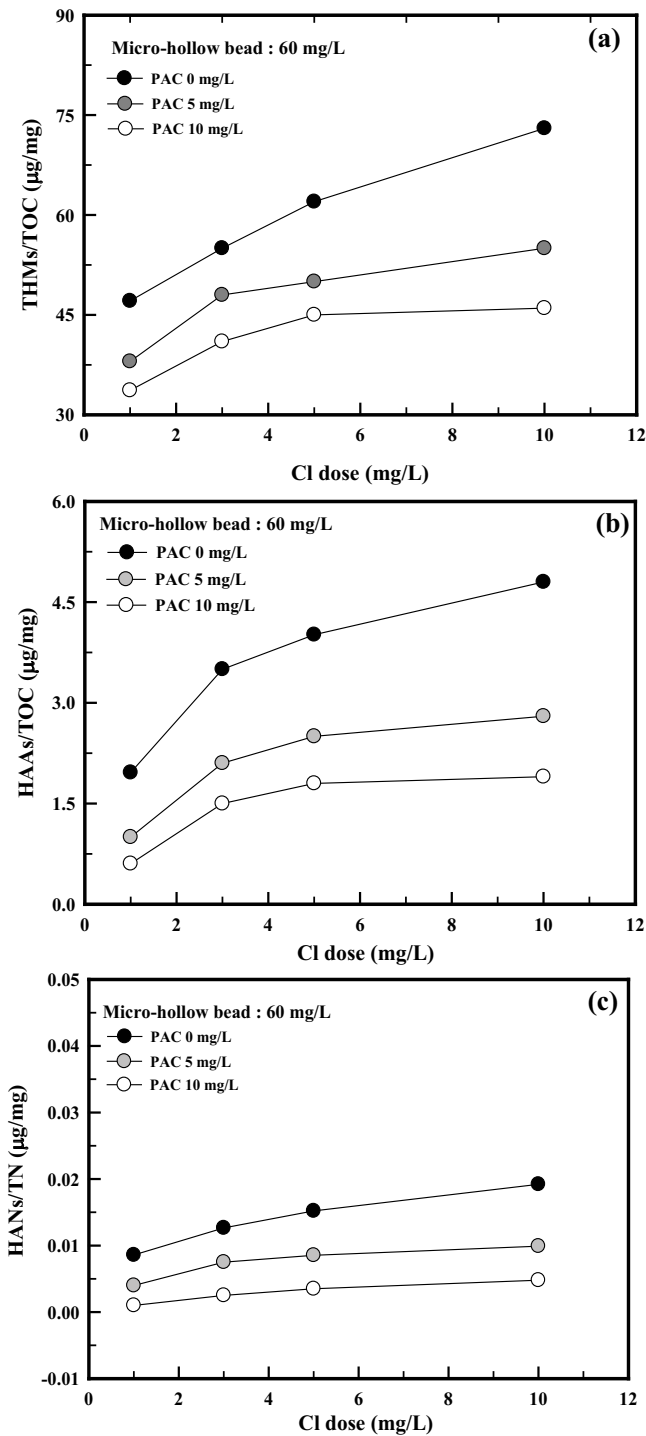


Fig. 7. Comparison of DBPs/precursors according to Cl and PAC dose. (a) THMs/TOC, (b) HAAs/TOC, and (c) HANs/TN.

after 7 d and increased to 1.2 and 1.4 times, respectively. With PAC 10 mg/L, the THMFP concentrations were constant over time, whereas HAAFP and HANFP concentrations increased with retention time. HANFP showed a high increase with retention time for 7 d, as reported previously [28]. HANFP is expected to increase the concentration in long piping which is connected with residual chlorine.

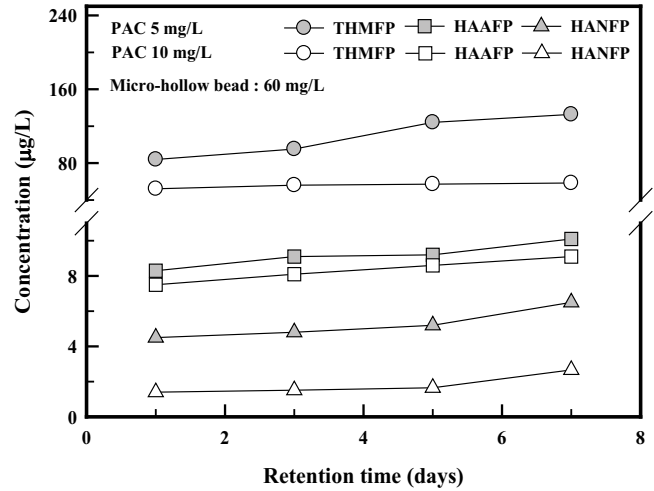


Fig. 8. Effect of THMFP, HAAFP, and HANFP by retention time.

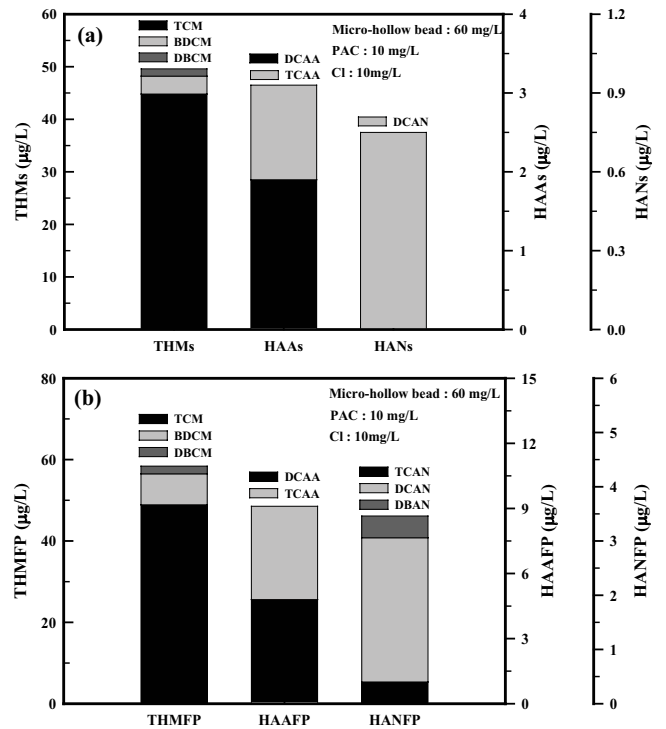


Fig. 9. Distribution of DBPs and DBPFP. (a) DBPs with no retention time and (b) DBPFP with retention time.

### 3.5.2. FP effect of THMs, HAAs, and HANs

To analyze the DBPFP of AOM, experiments were conducted with micro-hollow bead 60 mg/L, PAC 10 mg/L, and chlorine 10 mg/L according to retention time. As shown in Fig. 9a, three different DBPFPs were produced in the THMs; TCM detected the highest production of 44.8 µg/L, which was also reported in a previous study [29]. DCAA and TCAA concentrations from HAAs were 1.2 and 1.9 µg/L, respectively. DCAN detected from HANs was 0.75 µg/L. Fig. 9b shows the THMFP, HAAFP, and HANFP formations under chlorine 10 mg/L for 7 d. THMFP showed the highest concentration

with TCM at 48.9 µg/L. HAAFP showed BDCM and DBCM concentrations at 7.6 and 1.9 µg/L, respectively. THMFP and HAAFP showed similar results as those in Fig 9a, whereas HANFP detected three types, TCAN, DCAN, and DBAN. DCAN showed the highest concentration of 2.66 µg/L, whereas TCAN and DBAN showed concentrations of 0.4 µg/L respectively. TCAN and DBAN were not detected in HAN during chlorine retention time for 1 d, however various FPs were detected in HANFP when chlorine retention time was over 7 d.

#### 4. Conclusion

The MW distributions of EOM, IOM, and AOM were analyzed using the LC-OCD. EOM showed higher amounts in total organic concentrations. IOM had a higher ratio of LMW neutrals. Because IOM induced higher amounts of DBP, the removal of IOM without disrupting the chemical structure was a key factor for treatment. An analysis of the molecular distribution before and after chlorine treatment showed that the concentrations of large biopolymers and building blocks and humic substances decreased with chlorine treatment, whereas the concentrations of LMW neutrals and LMW acids increased. The addition of coagulants decreased the average size and concentration of particulate matter. The number of particles also decreased with the addition of micro-hollow beads. With chlorine, the average number of particles decreased, while the average particle size increased. These results were caused by the interaction of chlorine with AOM, where the chlorine disorganizes the organic material, resulting in various sizes of matter. With the addition of micro-hollow beads, DBP precursors such as TOC and TN are removed; this is because HAAs showed higher removal rates than THMs and HANs with the addition of micro-hollow beads. The addition of coagulants and chlorine also reduced the formation of DBPs. THMs/TOC and HAAs/TOC showed similar removal characteristics, with HANs/TN showing low removal. At PAC 10 mg/L, the retention time of chlorine increased the amount of HANFP, indicating that the retention time was an important factor for by-product formation. A long pipe network with an increased retention time of residual chlorine can increase the amount of HAN, which can adversely affect water quality. The formation of THMFP and HAAFP showed similar results to those for THMs and HAAs. However, with long chlorine exposure time with HANFP, HANFP detected two more formation potential such as TCAN and DBAN. It meant that TCAN and DBAN, as well as DCAN in the tap water, affected the DBP.

#### Acknowledgment

This paper is supported by the National Research Foundation (NRF-2018R1A2B2003059).

#### References

- [1] R. Henderson, S.A. Parsons, B. Jefferson, The impact of algal properties and pre-oxidation on solid-liquid separation of algae, *Water Res.*, 42 (2008) 1827–1845.
- [2] M. Maeng, N.K. Shahi, G.Y. Shin, H.J. Son, D.H. Kwak, S. Dockko, Formation characteristics of carbonaceous and nitrogenous disinfection by-products depending on residual organic compounds by CGS and DAF, *Environ. Sci. Pollut. Res.*, (2018) 1–10, doi: 10.1007/s11356-018-2919-9.
- [3] L.C. Hua, J.L. Lin, P.C. Chen, C. Huang, Chemical structures of extra- and intra-cellular algogenic organic matters as precursors to the formation of carbonaceous disinfection byproducts, *Chem. Eng. J.*, 328 (2017) 1022–1030.
- [4] J. Huang, N. Graham, M.R. Templeton, Y. Zhang, C. Collins, M. Mieuwenhuijsen, A comparison of the role of two blue-green algae in THM and HAA formation, *Water Res.*, 43 (2009) 3009–3018.
- [5] L. Li, N. Gao, Y. Deng, J. Yao, K. Zhang, Characterization of intracellular and extracellular algae organic matters (AOM) of *Microcystis aeruginosa*, and formation of AOM-associated disinfection byproducts and odor and taste compounds, *Water Res.*, 46 (2012) 1233–1240.
- [6] L.C. Hua, J.L. Lin, M.Y. Syue, C. Huang, P.C. Chen, Optical properties of algogenic organic matter within the growth period of *Chlorella* sp. and predicting their disinfection by-product formation, *Sci. Total Environ.*, 621 (2017) 1467–1474.
- [7] N. Zhang, C. Liu, F. Qi, B. Xu, The formation of haloacetamides, as an emerging class of N-DBPs, from chlor(am)ination of algal organic matter extracted from *Microcystis aeruginosa*, *Scenedesmus quadricauda* and *Nitzschia palea*, *RSC Adv.*, 7 (2017) 7679–7687.
- [8] I. Kristiana, D. Liew, R.K. Henderson, C.A. Joll, K.L. Linge, Formation and control of nitrogenous DBPs from Western Australian source waters: investigating the impacts of high nitrogen and bromide concentrations, *J. Environ. Sci.*, 58 (2017) 102–115.
- [9] M. Pivokonsky, J. Naceradska, I. Kopecka, M. Baresova, B. Jefferson, X. Li, R.K. Henderson, The impact of algogenic organic matter on water treatment plant operation and water quality: a review, *Crit. Rev. Env. Sci. Technol.*, 46 (2016) 291–335.
- [10] P. Xie, J. Ma, J. Fang, Y. Guan, S. Yue, X. Li, L. Chen, Comparison of permanganate peroxidation and preozonation on algae containing water: cell integrity, characteristics, and chlorinated disinfection by-product formation, *Environ. Sci. Technol.*, 47 (2013) 14051–14061.
- [11] K.C. Lee, B.C. Gegal, I.H. Choi, W.T. Lee, Formation characteristics and control of disinfection by products in a drinking water treatment plant using lake water, *J. Korea Soc. Environ. Eng.*, 37 (2015) 269–276.
- [12] S.A. Huber, A. Balz, M. Abert, W. Pronk, Characterisation of aquatic humic and non-humic matter with size-exclusion chromatography – organic carbon detection – organic nitrogen detection (LC-OCD-OND), *Water Res.*, 45 (2011) 879–885.
- [13] A. Gonzalez-Torres, A.M. Rich, R.K. Henderson, Evaluation of biochemical algal floc properties using reflectance Fourier-transform infrared imaging, *Algal Res.*, 27 (2017) 345–355.
- [14] S.H. So, I.H. Choi, H.C. Kim, S.K. Maeng, Seasonally related effects on natural organic matter characteristics from source to tap in Korea, *Sci. Total Environ.*, 592 (2017) 584–592.
- [15] M.R. Teixeira, M.J. Rosa, Comparing dissolved air flotation and conventional sedimentation to remove cyanobacterial cells of *Microcystis aeruginosa*: part 1: the key operating conditions, *Sep. Purif. Technol.*, 52 (2006) 84–94.
- [16] J.K. Edzwald, Dissolved air flotation and me, *Water Res.*, 44 (2010) 2077–2106.
- [17] M.R. Teixeira, M.J. Rosa, Comparing dissolved air flotation and conventional sedimentation to remove cyanobacterial cells of *Microcystis aeruginosa*: part 2: the effect of water background organics, *Sep. Purif. Technol.*, 53 (2007) 126–134.
- [18] I.G. Jeong, M.J. Yi, H. Zhao, S. Dockko, Characteristics of DBPs reduction of AOM by dissolved air flotation, *Desal. Wat. Treat.*, 54 (2015) 1436–1444.
- [19] P. Jarvis, P. Buckingham, B. Holden, B. Jefferson, Low energy ballasted flotation, *Water Res.*, 43 (2009) 3427–3434.
- [20] F. Ometto, C. Pozza, R. Whitton, B. Smyth, A.G. Torres, R.K. Henderson, P. Jarvis, B. Jefferson, R. Villa, The impacts of replacing air bubbles with microspheres for the clarification of algae from low cell-density culture, *Water Res.*, 53 (2014) 168–179.

- [21] C.S. Reynolds, D.A. Rogers, Seasonal variations in the vertical distribution and buoyancy of *Microcystis aeruginosa* Kütz. emend. Elenkin in Rostherne Mere, England, *Hydrobiologia*, 48 (1974) 17–23.
- [22] L. Li, Z. Wang, L.C. Rietveld, N. Gao, J. Hu, D. Yin, S. Yu, Comparison of the effects of extracellular and intracellular organic matter extracted from *Microcystis aeruginosa* on ultrafiltration membrane fouling: dynamics and mechanisms, *Environ. Sci. Technol.*, 48 (2014) 14549–14557.
- [23] D. Lee, M. Kwon, Y. Ahn, Y. Jung, S.N. Nam, I. Choi, J.W. Kang, Characteristics of intracellular algogenic organic matter and its reactivity with hydroxyl radicals, *Water Res.*, 144 (2018) 13–35.
- [24] T. Guo, Y. Yang, R. Liu, X. Li, Enhanced removal of intracellular organic matters (IOM) from *Microcystis aeruginosa* by aluminum coagulation, *Sep. Purif. Technol.*, 189 (2017) 279–287.
- [25] C.M.M. Bougeard, E.M. Goslan, B. Jefferson, S.A. Parsons, Comparison of the disinfection by-product formation potential of treated waters exposed to chlorine and monochloramine, *Water Res.*, 44 (2010) 727–740.
- [26] E.C. Wert, R.L. Rosario-ortiz, Intracellular organic matter from cyanobacteria as precursor for carbonaceous and nitrogenous disinfection byproduct, *Environ. Sci. Technol.*, 47 (2013) 6332–6340.
- [27] H.J. Son, C.U. Jeong, I.S. Kang, The relationship between disinfection by-product formation and characteristics of natural organic matter in the raw water for drinking water, *J. Korean Soc. Environ. Eng.*, 26 (2004) 457–466.
- [28] G. Hua, J. Kim, D.A. Reckhow, Disinfection byproduct formation from lignin precursors, *Water Res.*, 63 (2014) 285–295.
- [29] S.J. Cho, J.I. Peung, K.Y. Jung, D.H. Ahn, M.J. Shim, Evaluation on trihalomethanes (THMs) formation potential in raw water, *J. Korea Soc. Environ. Admin.*, 15 (2009) 7–15.